Original Open Access

Modeling and Biomechanical Analysis of Keratoconus

Seira Salimi [1], Ali Tavakoli Golpaygani [2*], Kamran Hassani[3]

1. Faculty of Medical Sciences and Technologies, Islamic Azad University, Science and Research Branch, Tehran, Iran.
2. Biomedical Engineering Research Group, Standard Research Institute, Karaj, Iran.
3. Faculty of Medical Sciences and Technologies, Islamic Azad University, Science and Research Branch, Tehran, Iran.

Abstract

Keratoconus is a non-inflammatory ocular disorder in which the cornea bulges in the shape of a cone. Therefore, this progressive disease will cause visual impairment. The precise aetiology of keratoconus is not well understood. Investigating the pathogenesis of keratoconus from a biomechanical point of view will determine which biomechanical factor plays the dominant role in keratoconus formation. In this study, using the finite element method, a three-dimensional model of the human cornea with anatomical dimensions was created, and hyperelastic isotropic properties were assigned to it. Then, the inner surfaces of the model were subjected to physiological intraocular pressure. This model was regarded as a healthy cornea and as a reference model. Then, two symmetric and asymmetric states of keratoconus were simulated. For this purpose, a circular region was created in the center of the cornea (for the symmetric state) or in one of its quarters (for the asymmetric state), and then, in this circular region (i.e., locally), the following operations were performed with three different intensities to simulate three different stages of symmetric/asymmetric keratoconus: 1) reducing the thickness, 2) weakening the mechanical properties, and 3) reducing the thickness and weakening the mechanical properties, simultaneously. By analyzing the displacements, it was found that the local weakening of the mechanical properties makes the cornea significantly steep in the area affected by the disease and causes keratoconus formation. Therefore, in keratoconus formation, the weakening of mechanical properties plays a primary role, and the reduction of thickness plays a secondary and auxiliary role.

Keywords Cornea, Keratoconus, Pathogenesis, Biomechanical Analysis, Finite Element Method.

1. Introduction

The eye is a very important and intricate structure in the human anatomy and consists of three layers. The cornea and the sclera form the exterior layer of the eyeball. The cornea and the sclera are interconnected at a specific region known as the limbus [1]. The cornea is an optically transparent tissue that envelops the anterior portion of the eye globe. It plays a pivotal role in the visual system. Specifically, it accounts for approximately two-thirds of the eye's refractive power. This tissue directs incoming light rays to the lens and, subsequently, to the retina [2]. In the central area of normal corneas, the orientation of collagen lamellae is predominantly in the nasal-temporal and inferior-superior directions. About 66% of the lamellae have this particular arrangement, and the remaining 33% have a random orientation. In the limbus region, there is a

* Correspondence:
atavakoli@standard.ac.ir

circumferential annulus composed of collagen fibrils that encircles the cornea [3].

Any change in the shape or the mechanical resistance of the cornea causes vision impairment. Changes in the shape or the mechanical resistance of the cornea occur in diseases where the intraocular pressure becomes abnormal (such as glaucoma) or in diseases that affect the structural and mechanical properties of the cornea (such as keratoconus) [4].

Keratoconus is a non-inflammatory, progressive disease. In this ocular disease, the cornea undergoes a weakening process as a result of abnormalities in its structure (such as the organization of collagen fibers) and/or its composition (such as the amount of proteoglycans, collagen, and keratocytes). Consequently, the cornea loses its ability to maintain its normal shape against the intraocular pressure (IOP). This inability causes the cornea to protrude outward and become cone-shaped; In this way, vision is impaired. The changes that occur in the structure and composition of the cornea often appear through changes in shape (or geometry such as thickness and curvature), mechanical properties, and optical properties [5]. In keratoconus disease, the orthogonal and regular arrangement of collagen fibers in the normal cornea is no longer present. Consequently, the cornea (stromal layer) loses its stiff anisotropic structure, its tissue transforms into an isotropic tissue, and its mechanical properties decrease [3].

There are different treatment methods (surgical and non-surgical) for the management of keratoconus. The choice of these methods depends on the stage of the disease as well as its rate of progression. These therapeutic interventions improve vision through three distinct mechanisms: 1) modification of corneal shape (contact lenses and intra-stromal corneal ring segments); 2) modification of corneal structure or composition (collagen cross-linking); and 3) transplantation of either the entirety of the cornea (penetrating keratoplasty) or specific layers of the cornea (deep anterior lamellar keratoplasty) [5], [6].

The precise aetiology of keratoconus is not well understood; however, it is believed that both environmental and genetic factors play a significant role in its formation. This disease usually occurs in isolation for patients; however, various studies have demonstrated that it can coexist with other diseases such as Down's syndrome, Leber's congenital amaurosis, atopic conditions, asthma, dermatitis, and collagen disorders such as Ehlers-Danlos syndrome, osteogenesis imperfecta, and mitral valve prolapse. Therefore, in relation to a portion of the etiology of keratoconus, at least in theory, it can be said: Considering the correlation between keratoconus and collagen disorders, it is concluded that the presence of an anomaly in the connective tissue may lead to the weakening of the collagen structure, and this weakness eventually leads to the formation of keratoconus. Furthermore, keratoconus can also manifest in individuals with a familial history of the disease [5]–[7]. In addition, various other factors can also cause the formation of keratoconus and its progression. These factors include long-term high intraocular pressure (IOP), sudden and forceful impacts, excessive and prolonged exposure to solar radiation, incorrect placement of contact lenses, rubbing the eyes, persistent irritation of the eyes, diminished strength of corneal tissue, and diminished mass of corneal tissue [2], [8].

Therefore, keratoconus can be defined as a pathological condition in which significant biological-mechanical alterations and interactions may occur [2], [8].

There are studies that have investigated this disease using the finite element method. Some of them have simulated this disease only by local weakening of the mechanical properties of the healthy cornea [3], [9], [10]. Some of them have compared the effect of "local reduction in thickness" and "local weakening of mechanical properties" in creating keratoconus using linear elastic models [2], [8]; However, in [2] the reduction in thickness and in [8] the weakening of mechanical properties have been introduced as the primary cause of the disease.

Therefore, it is not completely clear that the effect of "decreasing the thickness in the diseased area" overcomes the effect of "weakening the mechanical properties in the diseased area" for the formation of keratoconus? Or is the opposite true? In this study, we investigated the pathogenesis of keratoconus from a biomechanical point of view using a hyperelastic model. For this purpose, in the healthy cornea model, thickness and mechanical properties were reduced, "alone" and "both simultaneously". This procedure was performed for three different severities of the disease and in two symmetric and asymmetric states. Therefore, a total of one normal cornea model and eighteen keratoconus models were analyzed. The aim was to detect the initiating factor of this disease (thickness reduction or weakening of mechanical properties). Finally, by analyzing the displacements, it was identified in which of the models the slope (in the area affected by the disease) has increased; This increase in slope was considered as the formation of keratoconus. In this study, optical analysis was not performed, and the conclusion was based solely on displacement analysis.

2. METHODS

2.1. Modeling the healthy cornea

2.1.1. Geometry of the healthy cornea model

As we know, the limbus tissue affects the biomechanics of the cornea [9]. Therefore, in addition to the cornea, the limbus tissue was also considered. The geometric dimensions in the healthy model were as follows:

1) The anterior curvature of the sclera: 11.50 mm, and the anterior curvature of the cornea: 7.8 mm [11].

2) The posterior curvature of the cornea: 6.6 mm, the thickness of the cornea in the center: 0.55 mm, the thickness of the cornea at the point of connection to the limbus: 0.65 mm, and the diameter of the base of the cornea from the inside: 11 mm [2].

3) The diameter of the base of the cornea from the outside: 12 mm, the anterior curvature of the limbus: 6.50 mm, the posterior curvature of the limbus: 6 mm, and the length of the limbus: 0.5 mm [12].

4) junction of limbus and cornea: 0.65 mm, junction of limbus and sclera: 0.8 mm [13]. Figure 1 shows the dimensions considered for the healthy model.

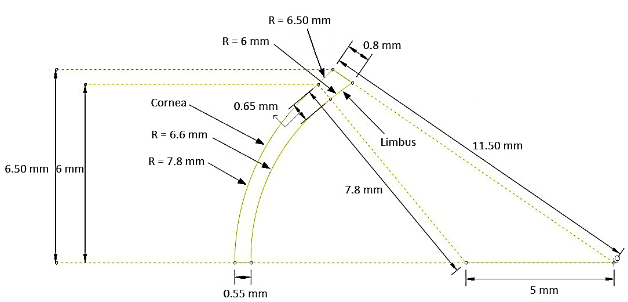

Fig 1. Dimensions considered for the healthy cornea. All dimensions are in millimeters (mm).

2.1.2. Mechanical properties of the healthy cornea model

As we said, in normal corneas, collagen fibers are oriented perpendicularly in the central region and circumferentially in the limbus region. However, when the corneal tissue undergoes degeneration, as observed in cases of keratoconus disease, This regular arrangement of collagen fibers that is present in the normal state will no longer exist (particularly in the cone area). Therefore, the presence of this disease causes the corneal tissue (stromal layer) to lose its stiff anisotropic structure, transform into an isotropic tissue, and decrease its mechanical properties. Since the arrangement of the majority of collagen fibers in keratoconic corneas is random and the ultimate goal of this study is to analyze keratoconic corneas, the "fiber-independent" and "isotropic" material model was used for the healthy cornea [3], [9], [10].

Therefore, in the healthy model, the behavior of corneal and limbus materials was simulated utilizing hyperelastic isotropic strain-energy functions. Both corneal and limbus tissues were simulated utilizing Neo-Hookean strain-energy functions, Nψ; See equation (1).

$$\psi_N = \frac{1}{D} \cdot \left(\frac{J_{el}^2 - 1}{2} - \ln(J_{el}) \right) + C_{10}^N . (\bar{I}_1 - 3) \qquad (1)$$

In relation (1), $\bar{\mathrm{I}}$ is the first invariant of the modified right Cauchy-Green tenso $\bar{C} = J_{el}^{-2/3}\, C$, J_{el} is the elastic volumen ratio, and $\frac{1}{D}$ is the bulk modulus. The material constants for the cornea and limbus tissues in the healthy model were as follows:

$C_{10}^N = 0.05$ MPa, and D = 0 MPa^{-1} [14].

2.1.3. Loading in the healthy cornea model

The physiological intraocular pressure (IOP) values are in the range of 10-24 mmHg, and their average value is equal to 15.6±2.7 mmHg [2]. Therefore, normal intraocular pressure (IOP) equal to 15 mmHg (0.002 MPa) was uniformly applied to the posterior surface of the cornea and limbus [14]. Figure 2 shows this loading.

2.1.4. Boundary conditions in the healthy cornea model

Since the cornea has a spherical shape, the spherical coordinate system (r, φ, θ) was used. The r-axis was considered perpendicular to the surface of the cornea, and the φ-axis was considered to be in line with the surface of the cornea. Figure 2 shows the spherical coordinate system used (the R-axis is equivalent to the r direction; the P-axis is equivalent to the φ direction; and the T-axis is equivalent to the θ direction) [2].

Empirical observations have shown that the limbus is not circumferentially stretchable (relatively). Furthermore, the majority of collagen fibrils at the limbus have a circumferential orientation and show considerable resistance to local stretch [2]. Therefore, the boundary conditions in the healthy model were defined as follows; in Figure 2:

1) Surface a: U_r and UR_r values were considered equal to zero.

2) Surface b: U_φ and UR_φ values were considered equal to zero.

2.1.5. Types of elements in the healthy cornea model

In the healthy model, all geometry was meshed using 10-node quadratic hybrid tetrahedral elements (C3D10H). Since the cornea is defined as an incompressible hyperelastic material, hybrid elements were used.

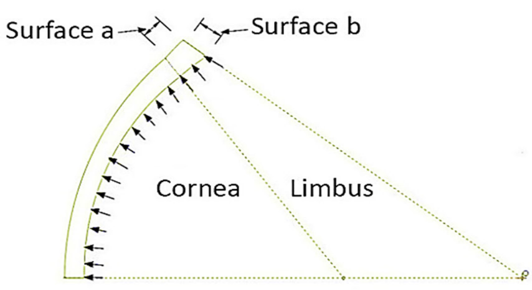

Fig 2. Loading and boundary conditions applied to the healthy cornea. Surface a was fixed in the radial direction, and surface b was fixed in the meridional direction.

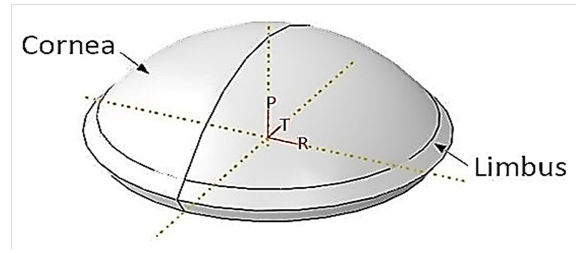

Fig 3. Spherical coordinate system used for the healthy cornea. The R-axis is equivalent to the r direction; the P-axis is equivalent to the φ direction; and the T-axis is equivalent to the θ direction.

2.2 Modeling of the keratoconic corneas

2.2.1. Determining the location and size of the patient region

The cone-shaped region in the keratoconic cornea can have different positions with respect to the central axis of the cornea. It can be completely symmetrical or completely asymmetrical with respect to this central axis, or it can be placed in a position between these two states [15]. In this study, two states, "completely symmetrical" and "completely asymmetrical", were selected to model keratoconic corneas:

1) Completely symmetrical state: the area affected by the disease is in the center of the cornea (Figure 4-A).
2) Completely asymmetrical state: the area affected by the disease is in one of the quarters of the cornea (Figure 4-B).

Regarding the size of the disease-affected area, previous finite element studies have considered the diameter of this area to be in the range of 2-4 mm [3], [8], [9], [14]. Therefore, according to the dimensions of the model that is investigated in this study, we considered the diameter of this area to be 2.50 mm.

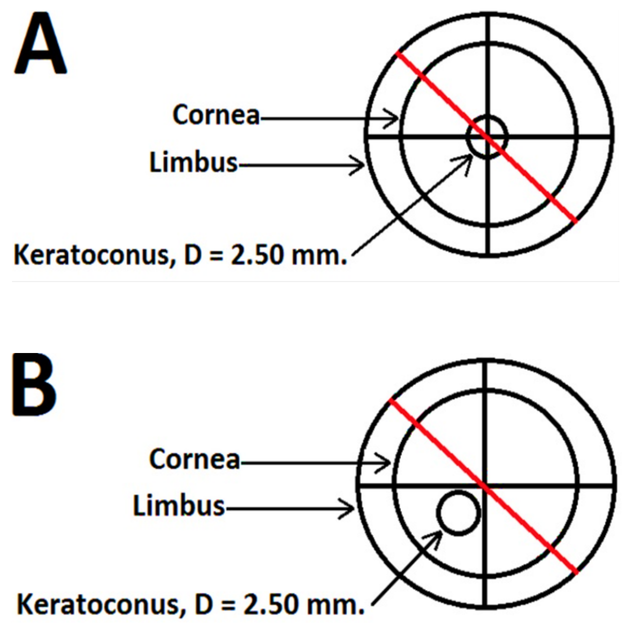

Fig 4. A: Completely symmetrical state, and B: Completely asymmetrical state. The red line shows the central axis of the cornea.

2.2.2. Loading, boundary conditions and types of elements in keratoconic cornea models

All these items were considered the same as the healthy cornea model.

2.2.3. Investigating the pathogenesis of keratoconus from a biomechanical point of view

Symmetric and asymmetric models were simulated in the following three ways:

1) only reducing the thickness in the area affected by the disease.
2) only the weakening of the mechanical properties in the area affected by the disease.
3) reducing the thickness and weakening the mechanical properties, simultaneously, in the area affected by the disease.

It is necessary to determine the separate effect of "thickness reduction in the area affected by the disease" and "weakening of mechanical properties in the area affected by the disease" on the shape of the cornea, as well as their combined effect. Figure 5 refers to this modeling.

2.2.4 | Simulation of disease progression

To simulate the progression of the disease, three different stages were considered. In other words, in the investigation of each state, "local reduction in thickness" and "local weakening of mechanical properties" were performed with three different intensities (Table 1).

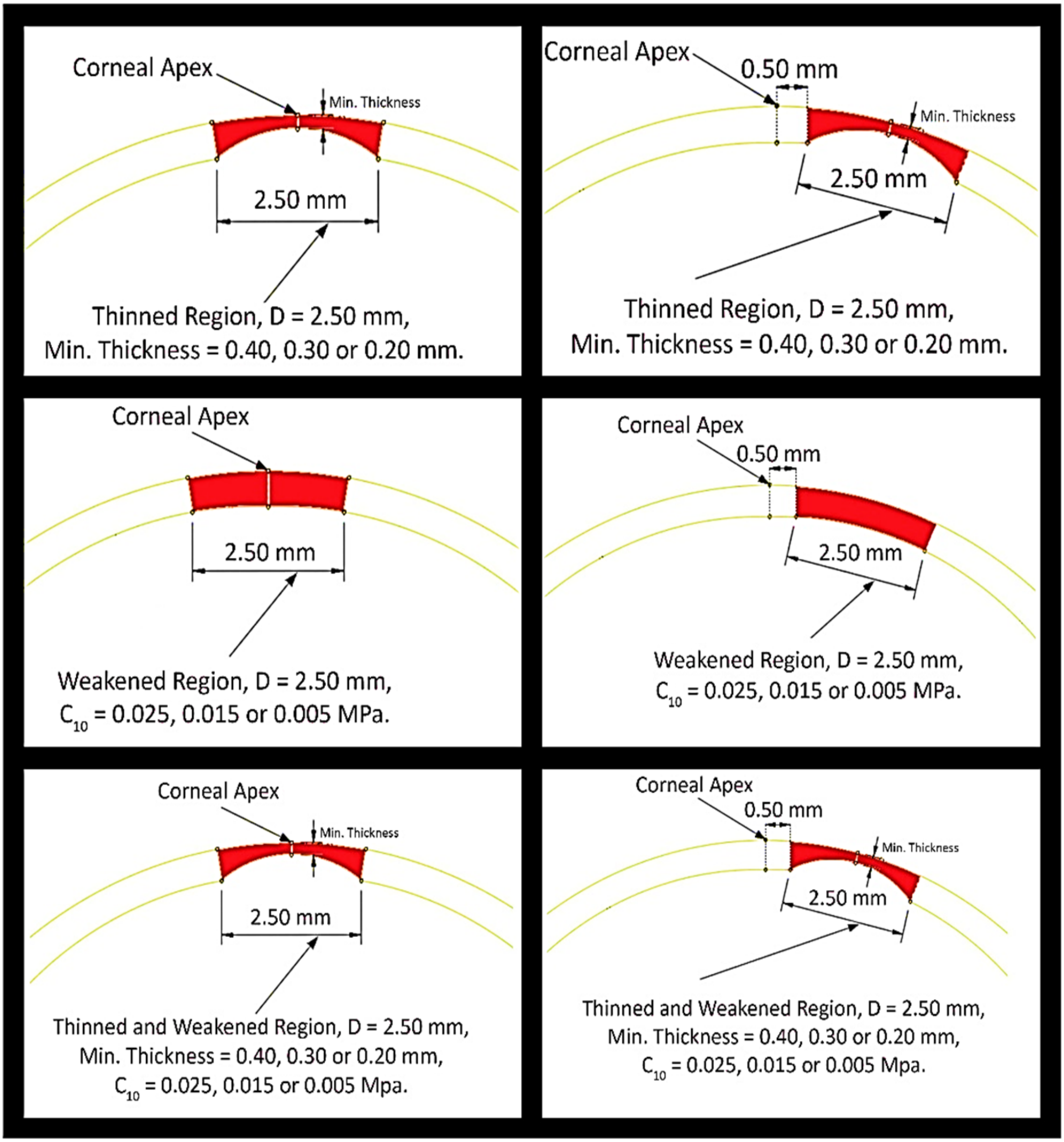

Fig 5. The two-dimensional view of symmetric (right column) and asymmetric (left column) models. First row: Reducing the thickness. Second row: Weakening of mechanical properties. Third row: Reducing the thickness and weakening the mechanical properties simultaneously.

2.3 | Type of analysis

A total of one normal cornea model and eighteen keratoconus models were analyzed. These models were investigated only from a biomechanical point of view, and optical analyses were not performed on them.

All analyses of this study were done in Abaqus software (Dassault Systèmes Simulia Corporation) (Ver. 2020) and statically.

Table 1. Simulation of keratoconus progression

Stages of the disease	Min. thickness in the disease-affected area (mm)	Value of C_{10} in the disease-affected area (MPa)
Stage 1	0.40	0.025 (50% reduction)
Stage 2	0.30	0.015 (70% reduction)
Stage 3	0.20	0.005 (90% reduction)

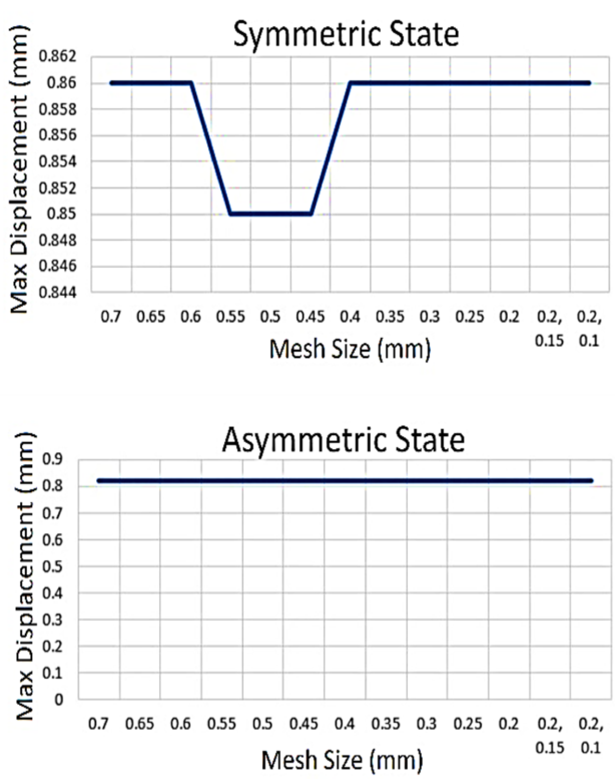

Fig 6. The results of the mesh independence analysis.

2.4 | Mesh independence analysis

To determine the optimal size of the elements, a mesh independence analysis was performed. This analysis was performed on the models that had the highest amount of thinning, That is, "in stage 3 and in symmetric and asymmetric states".

To perform this analysis, in each of the models, the size of the elements was changed from 0.70 to 0.20 mm. In addition, in each of the models, in two other steps, in the thin area of the cornea (i.e., locally), elements with sizes less than 0.20 mm were also considered; For this thin area, sizes of 0.15 mm and 0.10 mm were investigated (i.e., the remaining sections of each model were meshed with elements of 0.20 mm size).

Then, in each of the models, "maximum displacement values" were compared with each other at different steps.

According to the results of this analysis (Figure 6), we considered the size of the elements of all our models to be 0.20 mm, Without reducing the size of the elements locally in the thin area. Thus, 89052 elements were created in the healthy cornea model. The number of elements in the keratoconic models ranged from 86,723 to 90,830, depending on the model type.

3 | RESULTS

3.1 | Normal cornea

Figure 8 shows the contours of stress and displacement related to the simulation of the normal cornea. In addition, Figure 9 shows the stress and displacement diagrams along the central path of the cornea (Figure 7; on both the anterior and posterior surfaces of the cornea).

The displacement distribution diagram in Figure 9 shows that the maximum displacement is equal to 0.32 mm and occurs on the posterior surface of the corneal apex. The stress distribution diagram also shows that in the cornea region (without considering the limbus region), the maximum stress is approximately equal to 0.015 MPa and occurs near the apex region.

In addition, as mentioned in the study of Gefen et al., here too, the distribution of stress and displacement around the apex of the normal cornea exhibited a symmetrical pattern. This symmetrical pattern corresponds to the symmetry of the geometry of the model around the apex of the cornea [2].

Our results are consistent with the results related to modeling the normal cornea in the study of Gefen et al. [2]. Therefore, here too, the results related to the normal cornea were regarded as a reference for the results related to the modeling of keratoconic corneas.

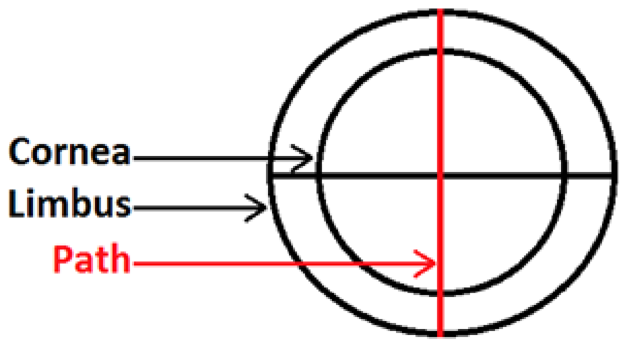

Fig 7. The red line shows the central path in the normal cornea.

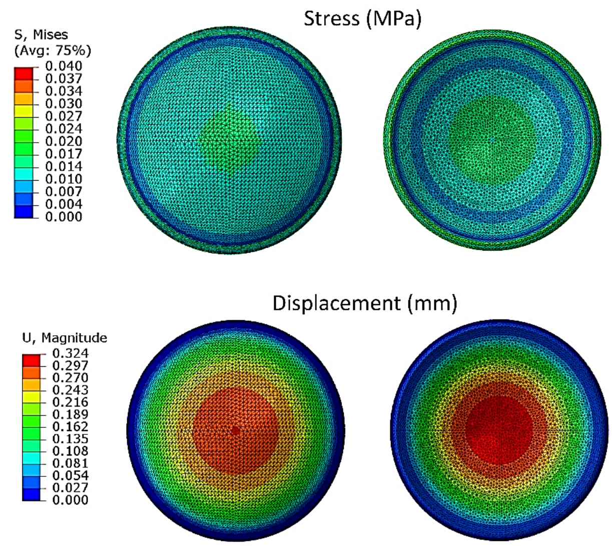

Fig 8. Stress (Mises) and displacement contours related to the normal cornea. The left column shows the anterior view of the cornea. The right column shows the posterior view of the cornea.

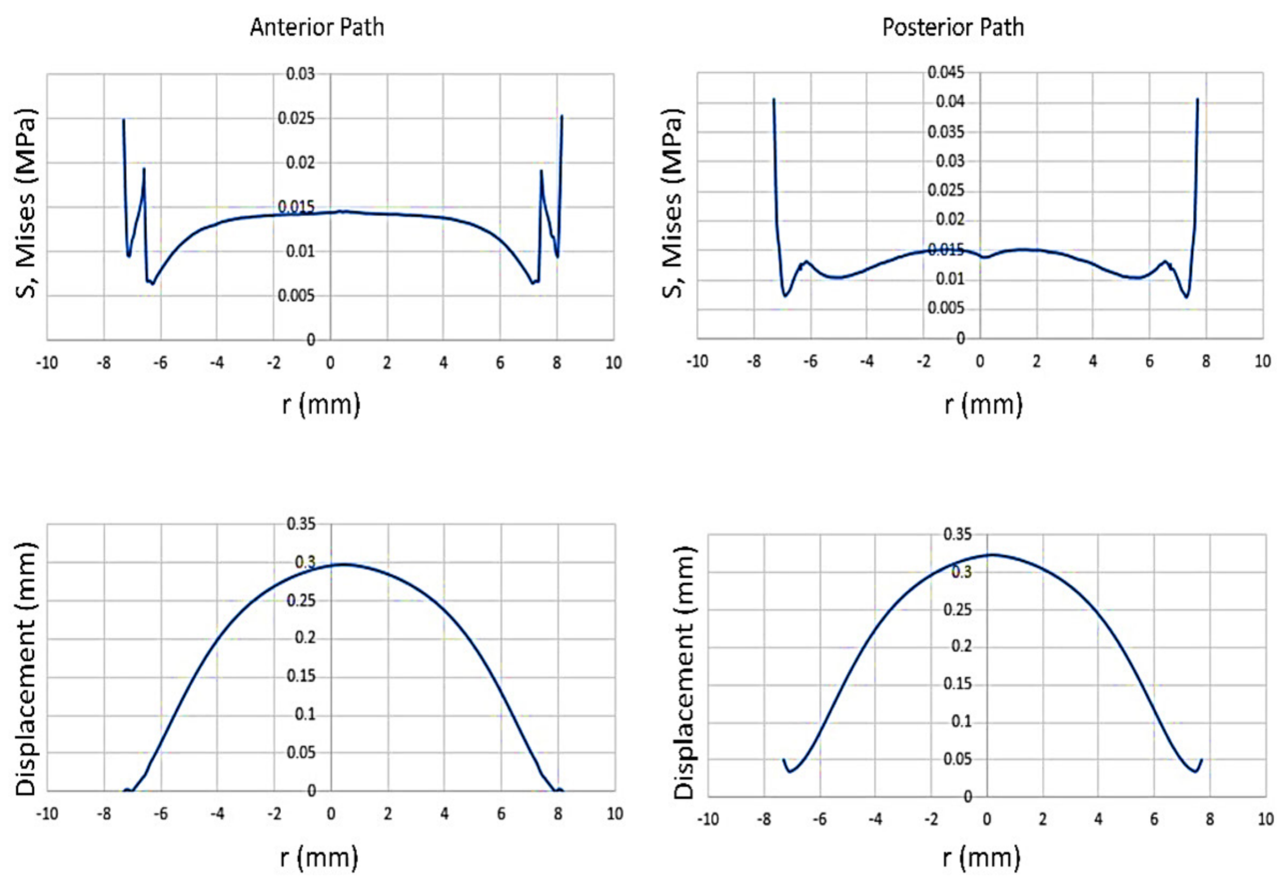

Fig 9. Diagrams of stress and displacement in the central path of the normal cornea. The diagrams are drawn on the anterior (left column) and posterior (right column) surfaces of this path.

3.2 | Keratoconic corneas

For each of the keratoconic corneas, stress and displacement contours were investigated. In addition, stress and displacement diagrams were drawn on the anterior and posterior paths passing through the center of the disease-affected area (i.e., on the anterior and posterior paths of the steep meridian; Figure 10).

From a clinical point of view, the maximum displacement of the cornea (especially in the cone area) has been accepted as a measure to determine the severity of keratoconus [2]. Therefore, in this analysis, maximum displacement was considered to evaluate the condition of keratoconus.

In all three states, the stress and displacement distributions were almost symmetric in symmetric keratoconus, and asymmetric in asymmetric keratoconus.

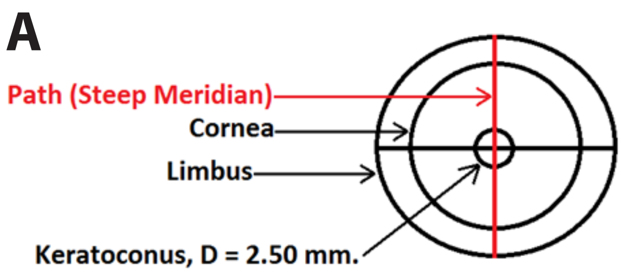

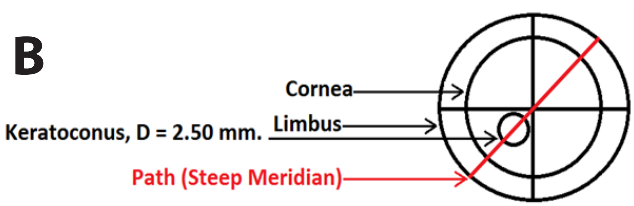

Fig 10. The red lines represent the anterior and posterior paths passing through the center of the disease-affected area in the symmetric (A) and asymmetric (B) states (i.e., the anterior and posterior paths of the steep meridians).

3.2.1. The effect of local reduction in thickness (in three different stages)

The stress contours (Figure 11) show that, compared to the stress distribution in the normal cornea, the stress in the thinned area has increased in each of the stages. The greater the severity of the disease (i.e., the lower the thickness of the thinned area), the greater the increase in stress (Figure 12).

The displacement contours (Figure 13) show that, compared to the distribution of displacement in the normal cornea, the displacement in the "peripheral sections of the thinned area" has increased slightly, and with the increase in the severity of the disease, this slight increase in displacement increases. But, the remarkable thing is that in the "central sections of the thinned area", the displacement has decreased, and with the increase in severity of the disease, this displacement reduction increases (Figure 14). It is clearly seen in the displacement diagrams that a noticeable bulge in the cornea is not created by only local reduction in the thickness; Rather, its surface morphology changes slightly, and only a little elevation and depression are created on its surface (Figure 14).

The analysis of the location and the maximum value of displacement for each of the symmetric and asymmetric states is as follows:

1) In the symmetrical state: in all stages, the maximum displacement is transferred to the periphery of the thin area (on the same posterior surface). The values of the maximum displacement in the symmetrical state are as follows: stage 1: 0.31 mm, stage 2: 0.31 mm, and stage 3: 0.32 mm.

2) In the asymmetric state: in all stages, the maximum displacement occurs at the same posterior surface of the corneal apex. The values of the maximum displacement in the asymmetric state are as follows: stage 1: 0.32 mm, stage 2: 0.33 mm, and stage 3: 0.34 mm.

As can be seen, in both symmetric and asymmetric states, regardless of the location of the maximum displacement, the values of the maximum displacement are not much different from the maximum displacement in the normal state (0.32 mm). That is, by reducing the thickness locally, a significant bulge in the cornea has not occurred.

3.2.2. The effect of local weakening of mechanical properties (in 3 different stages)

The stress contours (Figure 15) show that, compared to the stress distribution in the normal cornea, the stress in the weakened area has decreased in each of the stages; The greater the severity of the disease (the lower the C10 value in the weakened area), the greater the reduction in stress. On the other hand, in each of the stages, the stress on the border of the weakened area has increased; The greater the severity of the disease, the greater the increase in stress (Figure 16).

The displacement contours (Figure 17) show that, compared to the displacement distribution in the normal cornea, the displacement has increased in the weakened region. The greater the severity of the disease the greater the increase in displacement in the weak area (Figure 18).

In the displacement diagrams, it is clearly seen that with the local reduction in the mechanical properties of the cornea, a noticeable bulge is created in the cornea (Figure 18).

Based on the results of the analysis, the location and the maximum value of displacement for each of the symmetric and asymmetric states are as follows:

1) In the symmetrical state: the maximum displacement occurred on the same posterior surface of the corneal apex

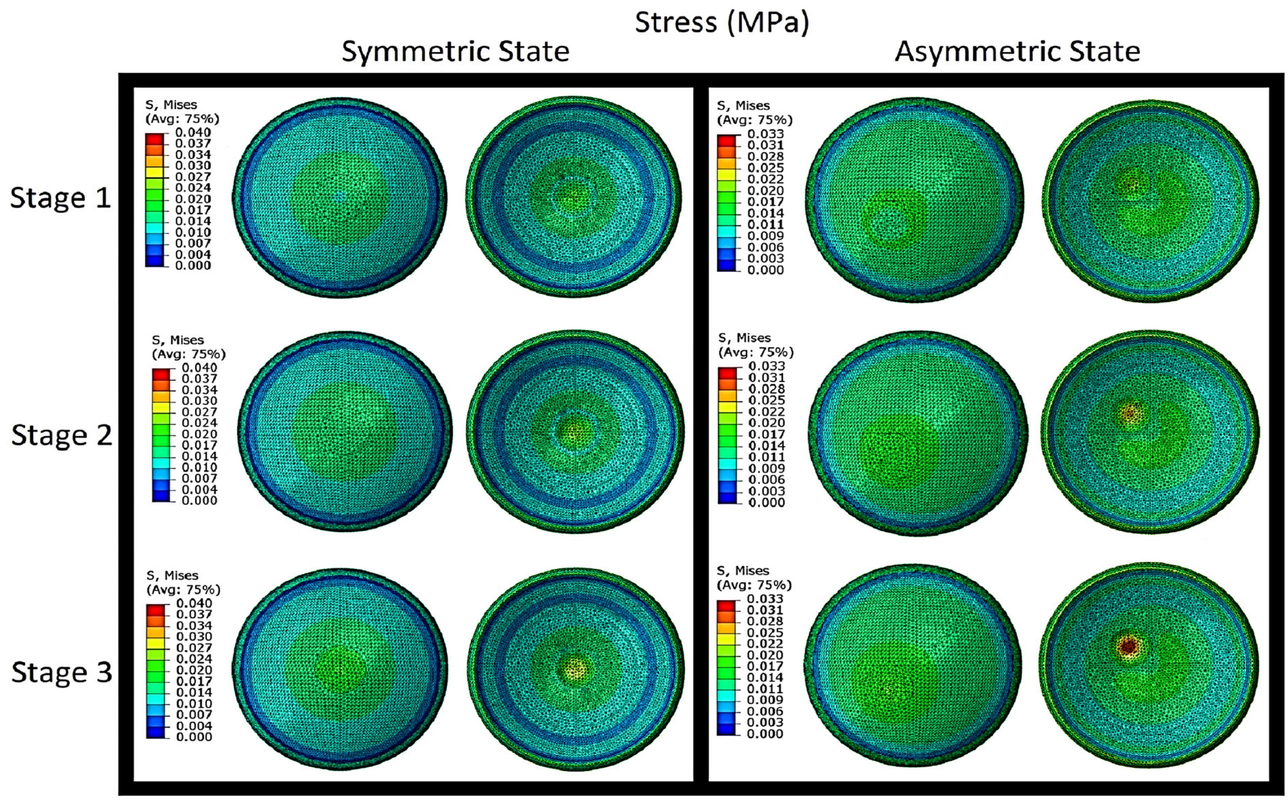

Fig 11. Stress (Mises) contours related to thickness reduction (locally) in the symmetric and asymmetric states. The results are related to three stages with different intensities. In each model, anterior and posterior views of the cornea are displayed.

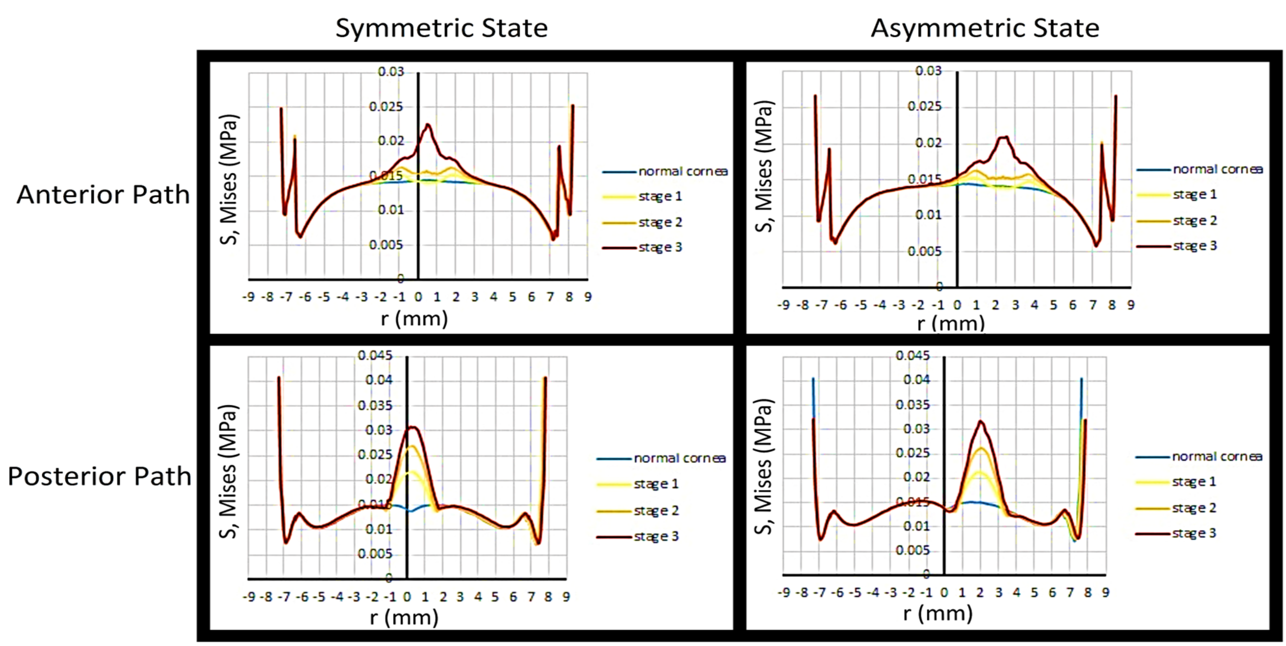

Fig 12. Stress (Mises) diagrams related to thickness reduction (locally) in the symmetric and asymmetric states. The diagrams are drawn on the anterior (row 1) and posterior (row 2) paths passing through the center of the disease-affected area. In each of the diagrams, the results related to the normal cornea and the three stages of the disease are comparable.

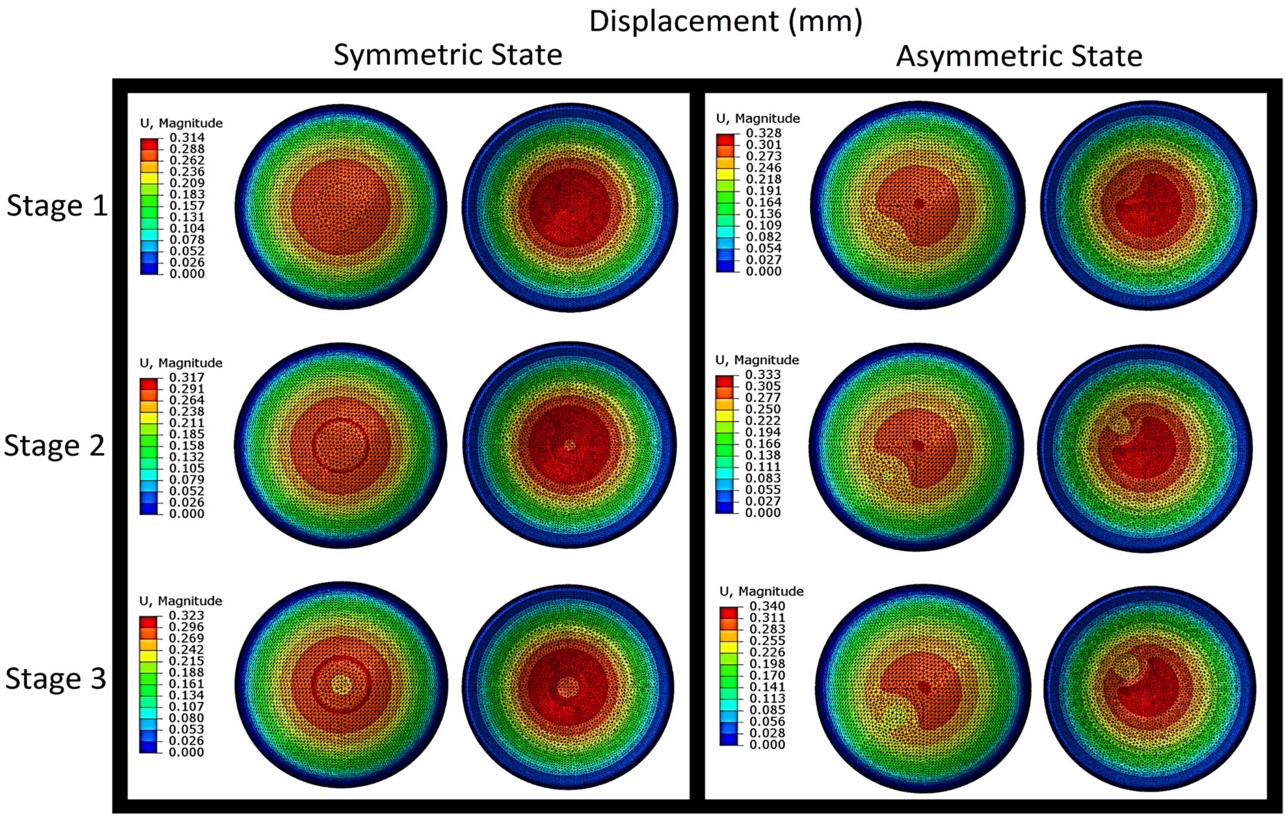

Fig 13. Displacement contours related to thickness reduction (locally) in the symmetric and asymmetric states. The results are related to three stages with different intensities. In each model, anterior and posterior views of the cornea are displayed.

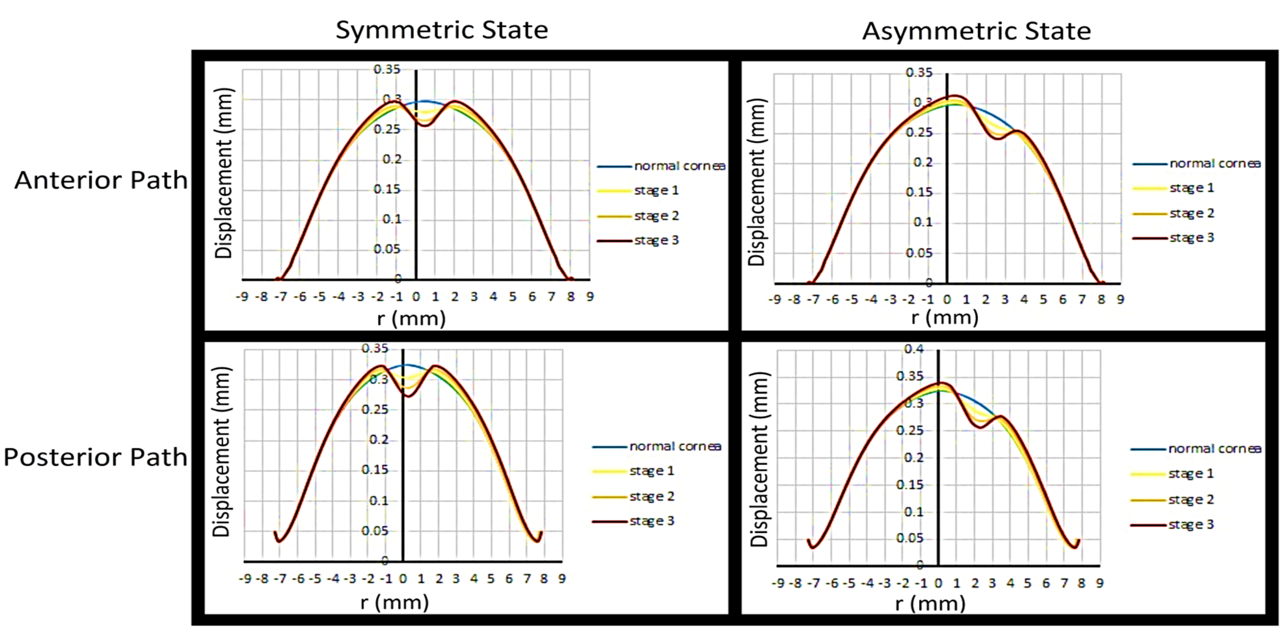

Fig 14. Displacement diagrams related to thickness reduction (locally) in the symmetric and asymmetric states. The diagrams are drawn on the anterior (row 1) and posterior (row 2) paths passing through the center of the disease-affected area. In each of the diagrams, the results related to the normal cornea and the three stages of the disease are comparable.

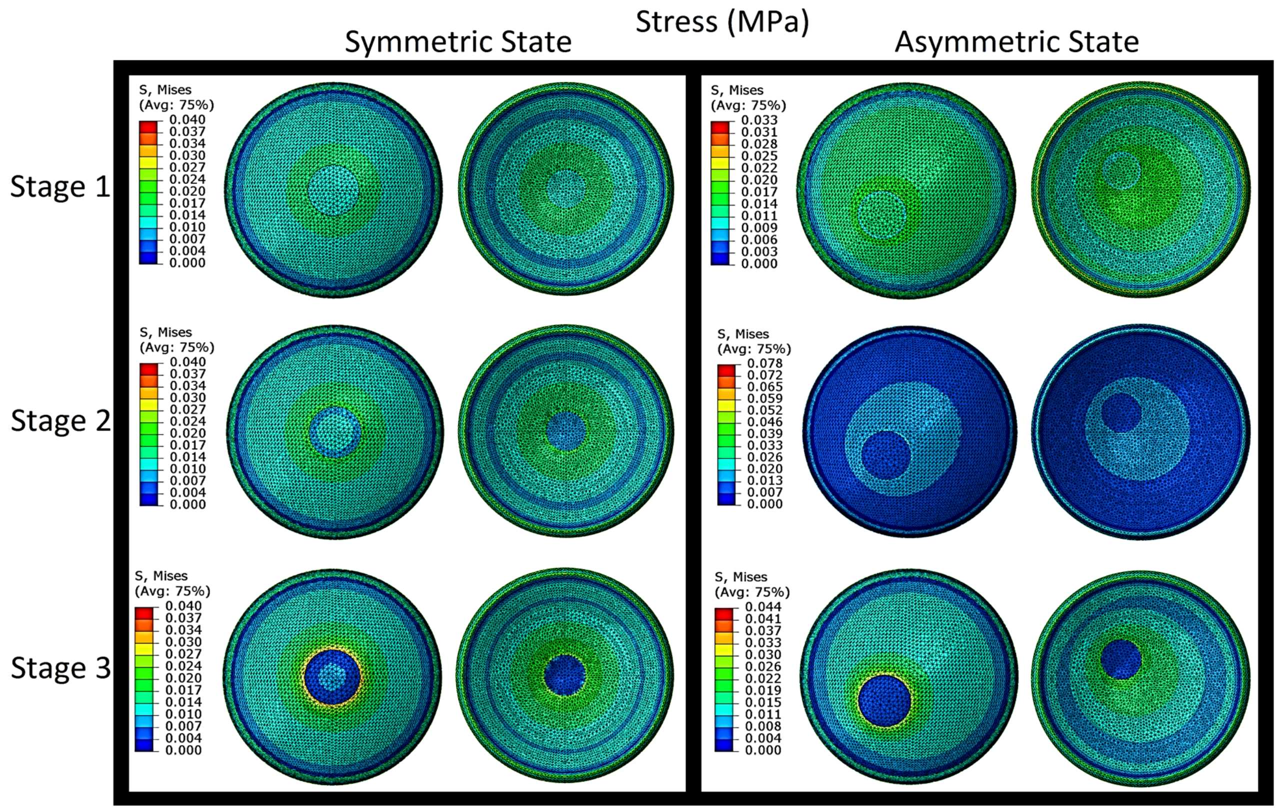

Fig 15. Stress (Mises) contours related to the weakening of mechanical properties (locally) in the symmetric and asymmetric states. The results are related to three stages with different intensities. In each model, anterior and posterior views of the cornea are displayed.

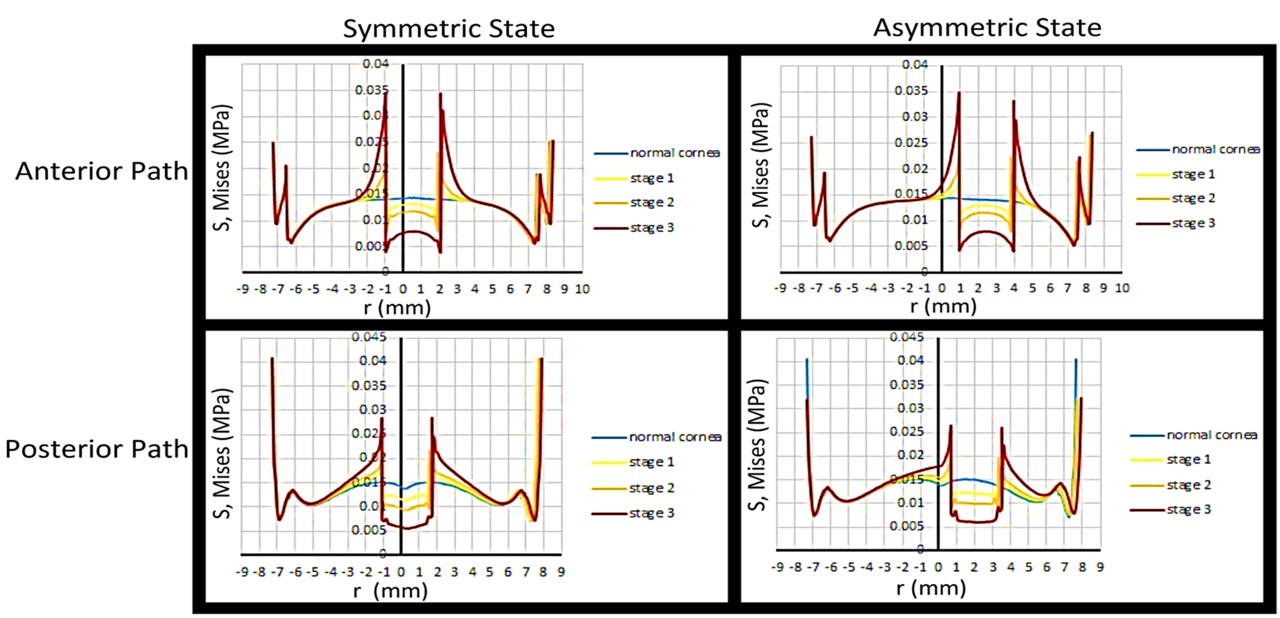

Fig 16. Stress (Mises) diagrams related to the weakening of mechanical properties (locally) in the symmetric and asymmetric states. The diagrams are drawn on the anterior (row 1) and posterior (row 2) paths passing through the center of the disease-affected area. In each of the diagrams, the results related to the normal cornea and the three stages of the disease are comparable.

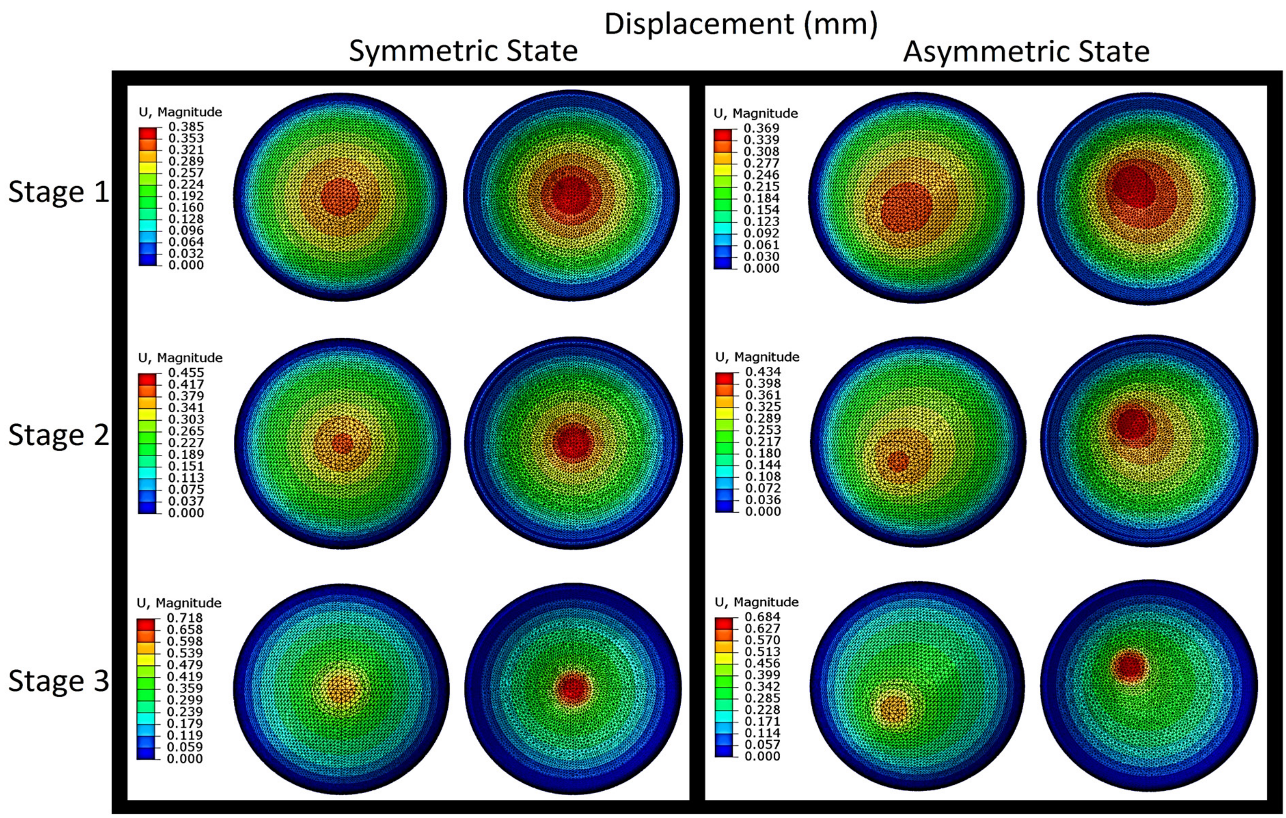

Fig 17. Displacement contours related to the weakening of mechanical properties (locally) in the symmetric and asymmetric states. The results are related to three stages with different intensities. In each model, anterior and posterior views of the cornea are displayed.

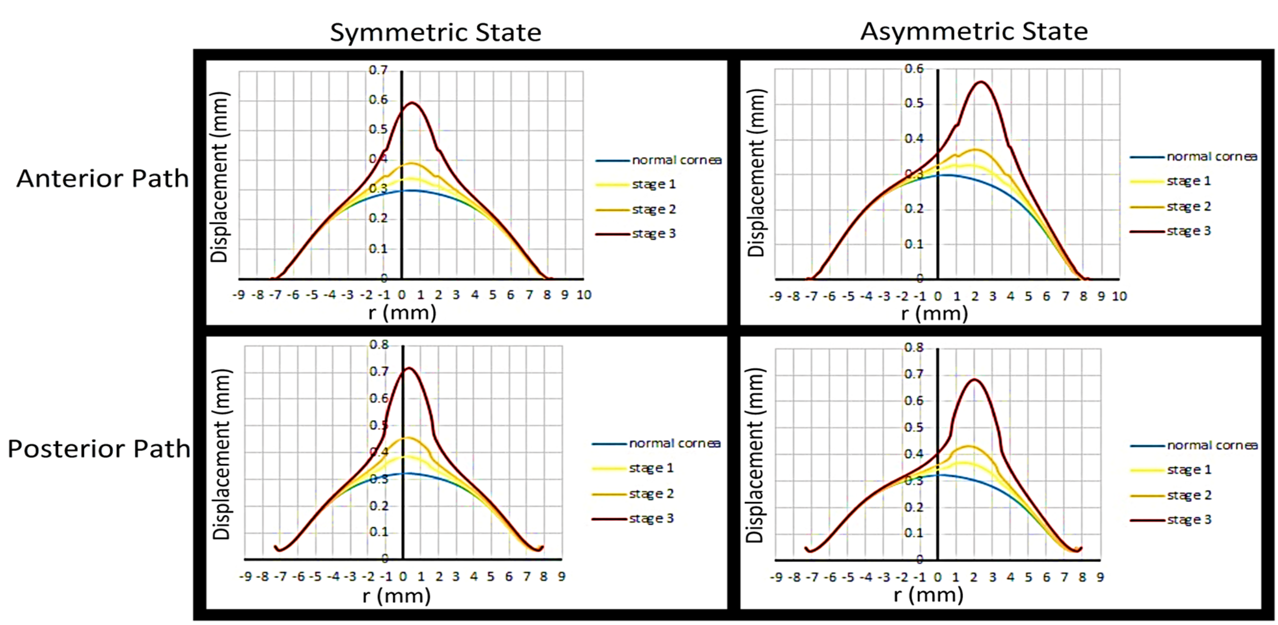

Fig 18. Displacement diagrams related to the weakening of mechanical properties (locally) in the symmetric and asymmetric states. The diagrams are drawn on the anterior (row 1) and posterior (row 2) paths passing through the center of the disease-affected area. In each of the diagrams, the results related to the normal cornea and the three stages of the disease are comparable.

(for all stages). The values of the maximum displacement in the symmetrical state are as follows: stage 1: 0.38 mm, stage 2: 0.45 mm, and stage 3: 0.71 mm.

2) In the asymmetric state: the maximum displacement is deflected into the weakened area (on its posterior surface). As the disease becomes more severe, the deflection of the maximum displacement into the weak area increases and moves towards the center of this area. The values of the maximum displacement in the asymmetric state are as follows: stage 1: 0.36 mm, stage 2: 0.43 mm, and stage 3: 0.68 mm.

As you can see, in both symmetric and asymmetric states, regardless of the location of the maximum displacement, the values of the maximum displacement are significantly different from the maximum displacement in the normal state (0.32 mm). That is, by weakening the mechanical properties locally, a significant bulge has occurred in the cornea.

3.2.3. The effect of reducing the thickness and weakening the mechanical properties, locally and simultaneously (in three different stages)

The stress contours (Figure 19) show that, compared to the stress distribution in the normal cornea, in each of the stages, the stress in the thinned and weakened area has decreased; The greater the severity of the disease (i.e., the lower the thickness of the thinned area and the lower the value of C10 in the weakened area), the almost greater the reduction in stress. On the other hand, in each of the stages, the stress on the border of the thinned and weakened area has increased; The greater the severity of the disease, the greater the increase in stress (Figure 20).

The displacement contours (Figure 21) show that, compared to the displacement distribution in the normal cornea, the displacement has increased in the thinned and weakened region. The greater the severity of the disease, the greater the increase in displacement in the thinned and weakened area (Figure 22). In the displacement diagrams, it is clearly seen that with the reduction in the thickness and the weakening of the mechanical properties, locally and simultaneously, a noticeable bulge is created in the cornea (Figure 22).

The location and the maximum value of displacement for each of the symmetric and asymmetric states are as follows:

1) In the symmetrical state: the maximum displacement occurred almost on the same posterior surface of the corneal apex (in all stages). The values of the maximum displacement in the symmetrical state are as follows: stage 1: 0.36 mm, stage 2: 0.43 mm, and stage 3: 0.86 mm.

2) In the asymmetric state: the maximum displacement is deflected into the thinned and weakened region (on its posterior surface). As the disease becomes more severe, the deflection of the maximum displacement into the thinned and weakened area increases and moves towards the center of this area; Thus, in stage 3, the maximum displacement occurred in the center of the thinned and weakened region (it is the thinnest point, too). The values of the maximum displacement in the asymmetric state are as follows: stage 1: 0.36 mm, stage 2: 0.42 mm, and stage 3: 0.82 mm.

As you can see, in both symmetric and asymmetric states, regardless of the location of the maximum displacement, the values of the maximum displacement are significantly different from the maximum displacement in the normal state (0.32 mm). That is, by reducing the thickness and weakening the mechanical properties, locally and simultaneously, a significant bulge has occurred in the cornea.

4. DISCUSSION

4.1. Normal cornea:

As mentioned, in this study, as in the study of Gefen et al., the distribution of stress and displacement around the apex of the normal cornea exhibited a symmetrical pattern; This symmetrical pattern corresponds to the symmetry of the geometry of the model around the apex of the cornea. However, it is worth noting that although the stress distribution in the normal cornea model was symmetrical, in the "real world", the stress distribution is not completely symmetrical, even in normal corneas [2].

4.2. Keratoconic corneas

4.2.1. The effect of local reduction in thickness (in three different stages)

From the observations, it was concluded that although the reduction in the thickness of the cornea locally caused an increase in the stress in the thin area (the stress increases more with the increase in the intensity of the thinning), but, it does not have a great effect on the bulging of the cornea and as a result the formation of keratoconus, and even It has reduced the displacement in the center of the thin area. The obtained results were consistent with the results of Roy Asher et al.'s study in 2014. They conducted a study to determine the pathogenesis of keratoconus based on biomechanical parameters. They investigated several different models with different conditions; In other words, they investigated the effect of reducing the thickness and weakening the mechanical properties of the cornea in different locations and with different intensities. One of the interesting results of their study was that when they weakened the mechanical properties locally in a section of the center of the cornea, more central protrusion was created; compared to when they reduced the thickness in the same section. That is, while the central corneal bulge was equal in the "normal" model and the "severely thin" model, the "severely weak" model had a much higher central bulge [8].

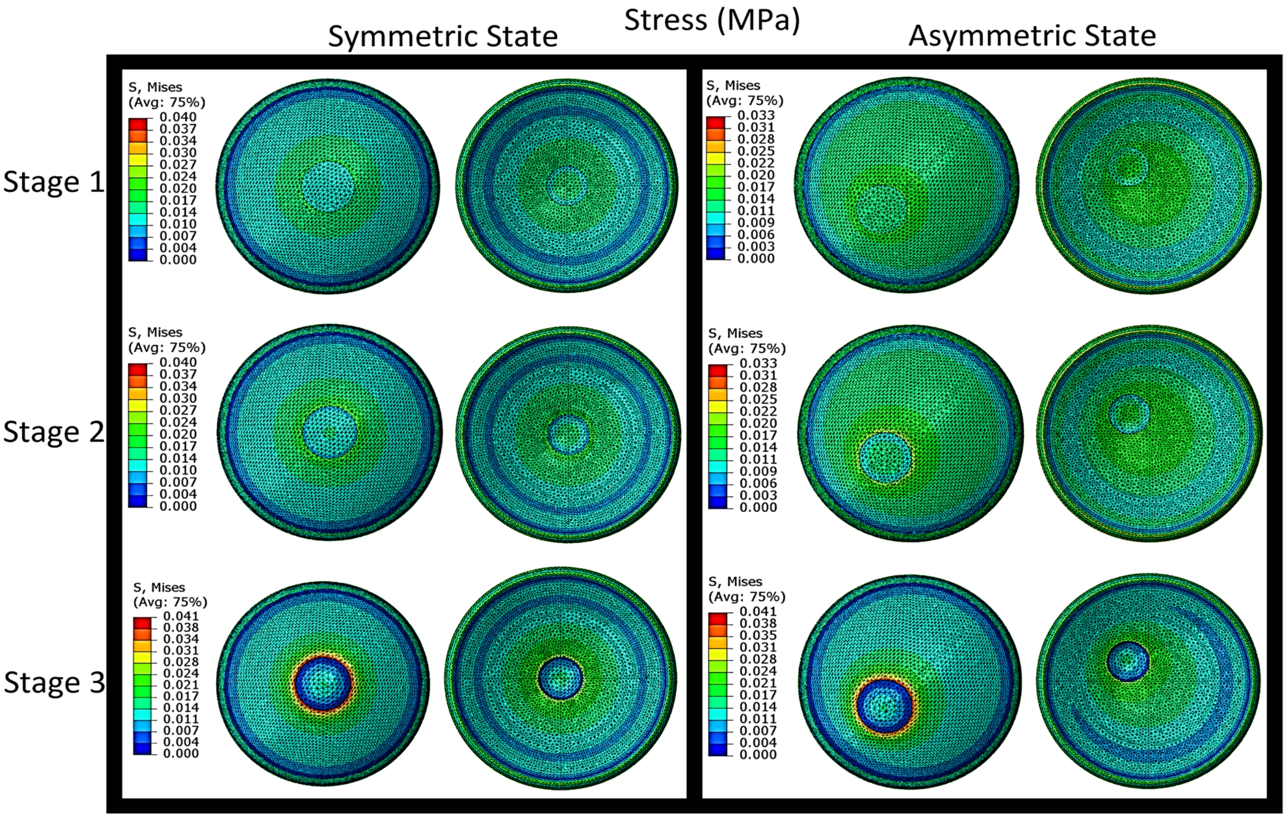

Fig 19. Stress (Mises) contours related to thickness reduction and weakening of mechanical properties (locally and simultaneously) in the symmetric and asymmetric states. The results are related to three stages with different intensities. In each model, anterior and posterior views of the cornea are displayed.

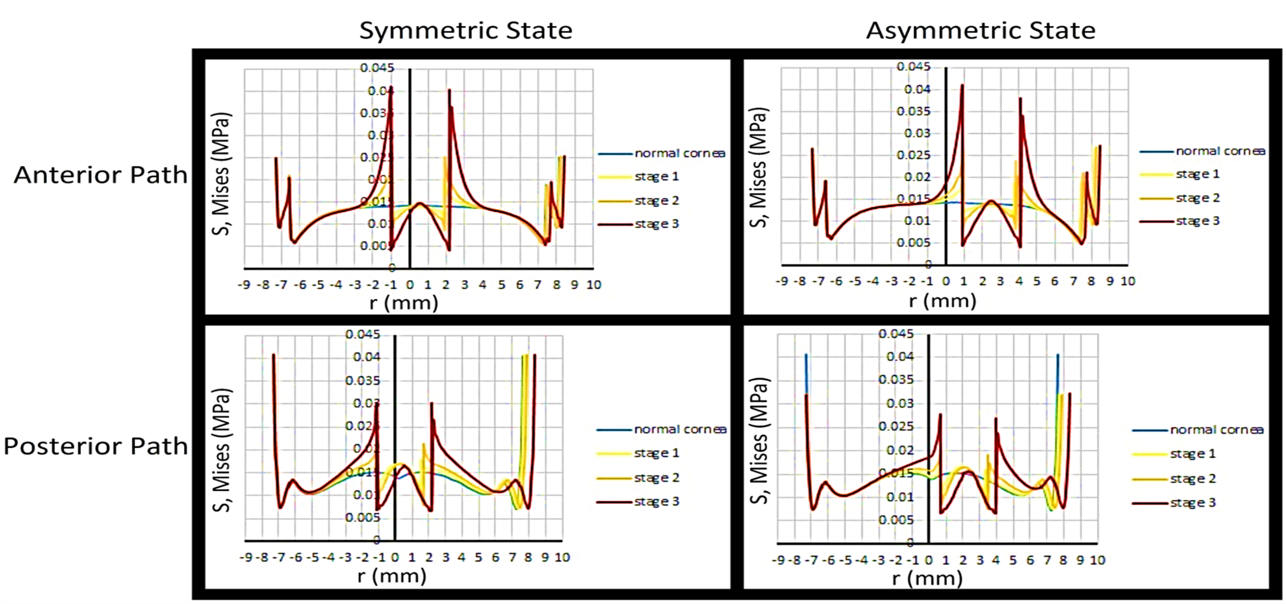

Fig 20. Stress (Mises) diagrams related to thickness reduction and weakening of mechanical properties (locally and simultaneously) in the symmetric and asymmetric states. The diagrams are drawn on the anterior (row 1) and posterior (row 2) paths passing through the center of the disease-affected area. In each of the diagrams, the results related to the normal cornea and the three stages of the disease are comparable.

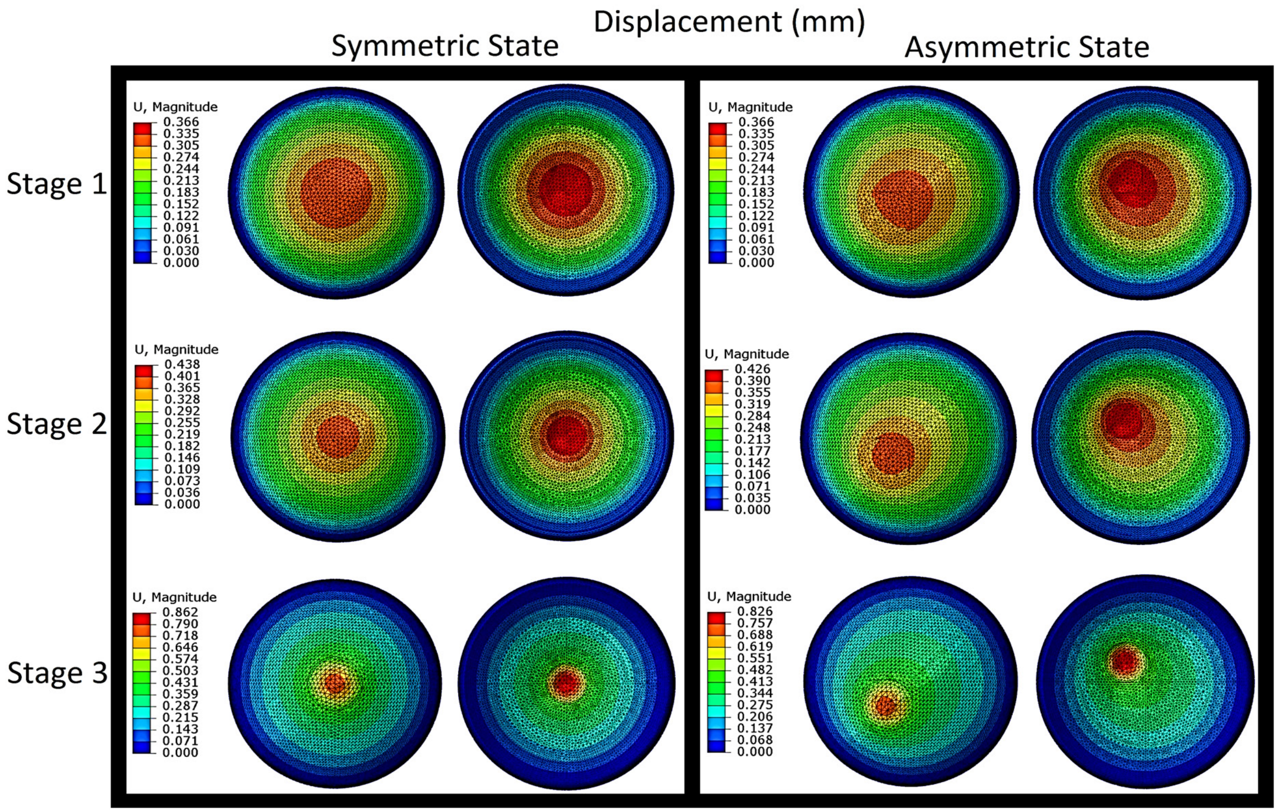

Fig 21. Displacement contours related to thickness reduction and weakening of mechanical properties (locally and simultaneously) in the symmetric and asymmetric states. The results are related to three stages with different intensities. In each model, anterior and posterior views of the cornea are displayed.

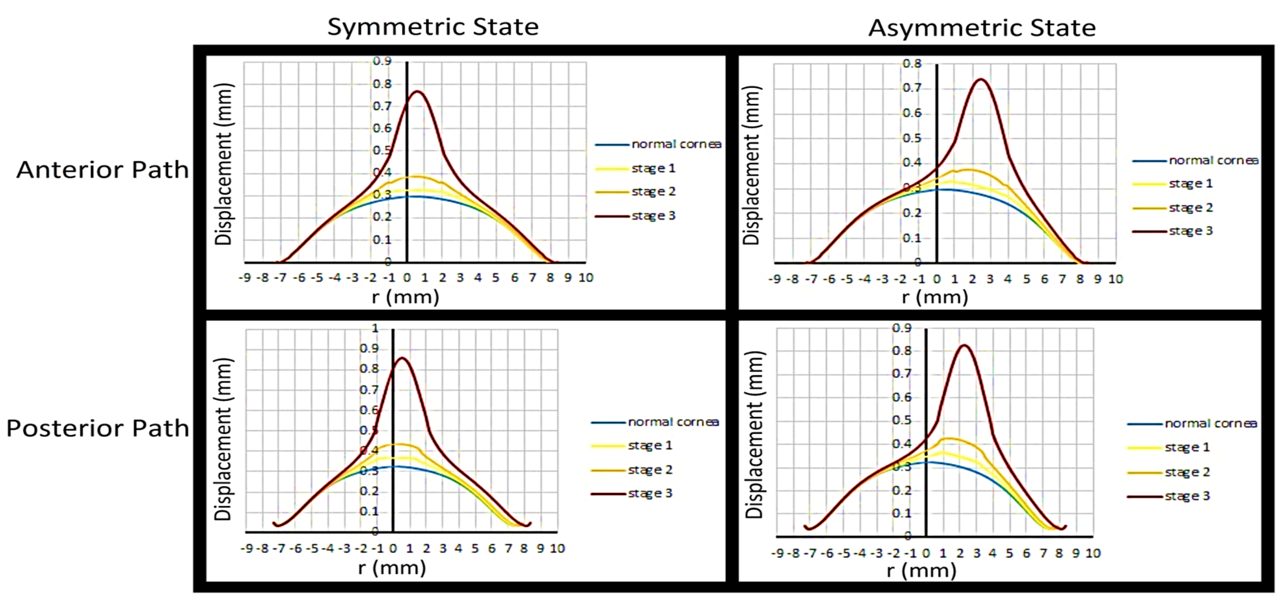

Fig 22. Displacement diagrams related to thickness reduction and weakening of mechanical properties (locally and simultaneously) in the symmetric and asymmetric states. The diagrams are drawn on the anterior (row 1) and posterior (row 2) paths passing through the center of the disease-affected area. In each of the diagrams, the results related to the normal cornea and the three stages of the disease are comparable.

Of course, in this analysis, although the local reduction in the thickness did not have a great effect on the formation of keratoconus, it caused the formation of elevation and depression on the surface of the cornea and its distortion; and this surface distortion can cause light refraction disorders and subsequently vision disorders.

4.2.2. The effect of local weakening of mechanical properties (in 3 different stages)

From the observations, it was concluded that the weakening of the mechanical properties of the cornea locally has caused an increase in the stress on the border of the weakened area, and with the increase in the intensity of the weakening of the mechanical properties, this increase in stress increases. This result was consistent with the result of Pandolfi and Manganiello's study in 2005. They defined a fiber-matrix model to represent the structure of the human cornea, then investigated the mechanical behavior of this cornea in keratoconus disease. To simulate keratoconus, they only weakened the mechanical properties in the area affected by the disease and did not reduce the thickness. To define the area affected by the disease, they considered a circular region (1.5 mm radius) in the inferior portion of the cornea, which was surrounded by an annular region (3 mm radius). The annular region was a transition region; That is, the mechanical properties were weakened to a lesser extent in the annular region than in the circular region. They observed that in a healthy cornea (at physiological intraocular pressure), the maximum Cauchy stress is located at the apex area of the cornea, and towards the limbus, while the thickness increases, the stress gradually decreases. In the keratoconic cornea, the maximum Cauchy stress occurred at the border of the degenerated area and was 80% higher compared to the healthy cornea [3]. In this study, as in study [3], the maximum stress in keratoconic models (in the cornea, that is, without considering the limbus area) occurred on the border of the degenerated area. In addition, it was concluded that the weakening of the mechanical properties of the cornea locally has reduced the stress in the weakened area; With the increase in the severity of the weakening of the mechanical properties, this stress reduction increases. These two results from this study, i.e., "decreasing stress in the weak zone" and "increasing stress on the border of the weak zone", were consistent with the results of the study by Carvlho et al. in 2009. To simulate keratoconus, they considered a circular area on the cornea model and reduced the mechanical properties of that area locally (without reducing the thickness). They observed that keratoconus has a great effect on the distribution of tension on the cornea; In other words, due to the presence of this degenerated area, the distribution of tension on the cornea underwent significant changes. The remarkable point in their study was that the von Mises pressures exhibited lesser magnitudes in the cone area. on the area surrounding the keratoconus, the tension increased. The reason for the increase in pressure on the surrounding area is that there is a substantial alteration in the corneal shape in this area. Conversely, in the central region of keratoconus, the tension persisted at a low level. The reduction in tensions in the central region of keratoconus can be attributed to the isotropic properties and lower elasticity values. The keratoconus had a great influence on the tension distribution over the cornea; In other words, due to the presence of this degenerated area, the tension distribution over the cornea underwent a substantial modification. It is important to highlight that over the keratoconus, compared to the surrounding regions, the surface tensions had lesser magnitudes. In the transition zone, that is, where the "non-keratoconic tissue" transformed into the "keratoconic tissue", the tension values heightened. The surface tension persisted at a low level in the center of the kratoconus. The behavior observed in this area can be elucidated by the isotropic properties and the lesser Young modules present in it [9]. On the other hand, we concluded that only by weakening the mechanical properties of the cornea locally, without local reduction in the thickness, a noticeable and significant bulge is created in the cornea. This result was consistent with the result of Sinha Roy et al.'s study in 2011. In their study, the clinical tomography was employed to capture the geometric data of a healthy eye belonging to a patient diagnosed with keratoconus (one eye of this keratoconic patient exhibited normal topography, and the other eye distinctly exhibited the presence of keratoconus). Subsequently, a three-dimensional finite element model of this eye was produced. They evaluated the effect of the "weakening of the mechanical properties of the cornea locally" on the etiology and subsequent progression of keratoconus. They simulated the progression of the keratoconus by using graded and localized reductions in the elastic modulus. In the area where the mechanical properties had reduced, the curvature experienced a nonlinear increase from 44 diopters to 52 diopters (This alteration occurred with a 45% reduction in the mechanical properties). Consequently, they concluded that keratoconus can occur only with a gradual decrease in elastic modulus, i.e., without any decrease in thickness [10], [16]. Additionally, the result of this analysis, i.e., the creation of a noticeable and significant bulge in the cornea only by weakening the mechanical properties of the cornea locally, without a local reduction in thickness, was consistent with the result of the study by Roy Asher et al. in 2014. As we explained earlier, they conducted a study to determine the pathogenesis of keratoconus based on biomechanical parameters. They observed that while the central corneal bulge was equal in the "normal" model and the "severely thin" model, the "severely weak" model had a much higher central bulge [8].

4.2.3. The effect of reducing the thickness and weakening the mechanical properties, locally and simultaneously (in three different stages)

From the observations, it was concluded that the changes caused by "thickness reduction and weakening of the mechanical properties, locally and simultaneously" in the patterns of the stress and displacement distributions of the cornea are very similar to the changes caused only by "weakening of the mechanical properties locally" in these patterns.

But, here, in stage 3, the values of maximum displacement are slightly higher in the disease-affected area; Because, local reduction in the thickness has aggravated the condition of the disease. Therefore, it is concluded that the main factor in the formation of keratoconus is the weakening of the mechanical properties of the cornea. In other words, reducing the thickness plays an auxiliary and supplementary role and has a secondary effect; That is, it only causes the symptoms of the disease to intensify.

5. LIMITATIONS

In this study, certain simplifications were applied to the models. It is necessary to pay attention to these simplifications during the process of analyzing and comprehending the outcomes; In future studies, these simplifications can be reduced, and more realistic results can be obtained. These simplifications are as follows:

1) In this study, optical analysis was not performed on the models, and the conclusion was based solely on the analysis of displacements. In future studies, more reliable results can be obtained by performing optical analysis on the models.

2) The dimensions considered for the geometry of the cornea and limbus were anatomical dimensions, while these dimensions can be different in different people. Therefore, more reliable results can be obtained by using patient-specific geometries and their "stress-free configuration". Furthermore, in actuality, the configuration of the central cornea exhibits an elliptical form. But, in this study, It was postulated that the central cornea possesses a hemispherical shape. Nevertheless, it should be acknowledged that the hemispherical shape closely approximates the ellipsoidal shape of the cornea [2].

3) In this study, scleral modeling was not performed. However, it is important to note that the scleral tissue supports the corneal tissue in a compliant manner and therefore has an effect on the biomechanical response of the corneal tissue [3], [9].

4) Since this study is not patient-specific, a hyperelastic material with general characteristics was used to model the cornea and limbus, and the elastic constants were reduced in the areas affected by the disease. However, as mentioned in the study of Lago et al. in 2015, Today, using in-vivo methods [17], [18], the biomechanical behavior of the cornea can be determined in each person; In other words, today, it is possible to obtain patient-specific biomechanical properties. Therefore, if these methods are used in simulations, more realistic results can be achieved [19].

5) In this study, the corneal and limbus tissues were considered isotropic materials. Because, in keratoconic corneas, the orthogonal distribution of collagen fibers in the cornea and their circumferential distribution in the limbus are disturbed [3]. As mentioned in the study of Lago et al. in 2015, disorganization of collagen fibers in keratoconus causes a "heterogeneous behavior" in the corneal tissue. Therefore, this issue renders the calculation of the exceedingly irregular biomechanical model of keratoconic corneas quite challenging. Hence, in this study, as in the study by Lago et al. in 2015, it was assumed that the tissue of the keratoconic cornea is an isotropic material (i.e., the mechanical properties remain constant across the entire tissue). In order to increase the precision of the outcomes in future studies, an improved biomechanical model can be employed that describes the anisotropic behavior in keratoconic corneas more accurately [19].

6. CONCLUSION

In this study, using the finite element method, we investigated and analyzed the pathogenesis of keratoconus from a biomechanical point of view. It was concluded that weakening the mechanical properties of the cornea locally plays the primary role in the occurrence of keratoconus. In other words, the local reduction in the thickness of the cornea plays an auxiliary and supplementary role and has a secondary effect; That is, it only causes the symptoms of the disease to intensify.

Funding

This research received no specific grant from any funding agency in the public, commercial, or not-for-profit sectors.

Declarations

Ethics approval and consent to participate
Not applicable.

Consent for publication
Not applicable.

Competing interests
The authors declare that they have no competing interests.

Received: Jan. 2024 Accepted: Mar. 2024
Published online: Mar. 2024

DOI: 10.22034/ASAS.2024.440836.1051

REFERENCES

[1] C. E. Willoughby, D. Ponzin, S. Ferrari, A. Lobo, K. Landau, and Y. Omidi, "Anatomy and physiology of the human eye: effects of mucopolysaccharidoses disease on structure and function–a review," Clin. Experiment. Ophthalmol., vol. 38, pp. 2–11, 2010, doi.org/10.1111/j.1442-9071.2010.02363.x.
[2] A. Gefen, R. Shalom, D. Elad, and Y. Mandel, "Biomechanical analysis of the keratoconic cornea," J. Mech. Behav. Biomed. Mater., vol. 2, no. 3, pp. 224–236, 2009, doi.org/10.1016/j.jmbbm.2008.07.002.
[3] A. Pandolfi and F. Manganiello, "A model for the human cornea: constitutive formulation and numerical analysis," Biomech. Model. Mechanobiol., vol. 5, no. 4, pp. 237–246, 2006, doi.org/10.1007/s10237-005-0014-x.
[4] A. Benoit, G. Latour, S.-K. Marie-Claire, and J.-M. Allain, "Simultaneous microstructural and mechanical characterization of human corneas at increasing pressure," J. Mech. Behav. Biomed. Mater., vol. 60, pp. 93–105, 2016, doi.org/10.1016/j.jmbbm.2015.12.031.
[5] R. Ambekar, K. C. Toussaint Jr, and A. W. Johnson, "The effect of keratoconus on the structural, mechanical, and optical properties of the cornea," J. Mech. Behav. Biomed. Mater., vol. 4, no. 3, pp. 223–236, 2011, doi.org/10.1016/j.jmbbm.2010.09.014.
[6] Y. S. Rabinowitz, "Keratoconus," Surv. Ophthalmol., vol. 42, no. 4, pp. 297–319, 1998, doi.org/10.1016/S0039-6257(97)00119-7.
[7] H. R. Vellara and D. V Patel, "Biomechanical properties of the keratoconic cornea: a review," Clin. Exp. Optom., vol. 98, no. 1, pp. 31–38, 2015, doi.org/10.1111/cxo.12211.
[8] R. Asher, A. Gefen, E. Moisseiev, and D. Varssano, "Etiology of Keratoconus: proposed biomechanical pathogenesis," Silico Cell Tissue Sci., vol. 1, no. 1, p. 3, 2014, doi.org/10.1186/2196-050X-1-3.
[9] L. A. Carvalho et al., "Keratoconus prediction using a finite element model of the cornea with local biomechanical properties," Arq. Bras. Oftalmol., vol. 72, no. 2, pp. 139–145, 2009, doi.org/10.1590/S0004-27492009000200002.
[10] A. S. Roy and W. J. Dupps, "Patient-specific computational modeling of keratoconus progression and differential responses to collagen cross-linking," Invest. Ophthalmol. Vis. Sci., vol. 52, no. 12, pp. 9174–9187, 2011, doi.org/10.1167/iovs.11-7395.
[11] J. R. Crouch, J. C. Merriam, and E. R. Crouch, "Finite element model of cornea deformation," in International Conference on Medical Image Computing and Computer-Assisted Intervention, 2005, pp. 591–598, doi.org/10.1007/11566489_73.
[12] E. Lanchares, B. Calvo, J. A. Cristóbal, and M. Doblaré, "Finite element simulation of arcuates for astigmatism correction," J. Biomech., vol. 41, no. 4, pp. 797–805, 2008, doi.org/10.1016/j.jbiomech.2007.11.010.
[13] R. Grytz and G. Meschke, "A computational remodeling approach to predict the physiological architecture of the collagen fibril network in corneo-scleral shells," Biomech. Model. Mechanobiol., vol. 9, no. 2, pp. 225–235, 2010, doi: 10.1007/s10237-009-0173-2.
[14] J. Flecha-Lescún, B. Calvo, J. Zurita, and M. Á. Ariza-Gracia, "Template-based methodology for the simulation of intracorneal segment ring implantation in human corneas," Biomech. Model. Mechanobiol., vol. 17, no. 4, pp. 923–938, 2018, doi: 10.1007/s10237-018-1013-z.
[15] L. Torquetti, R. F. Berbel, and P. Ferrara, "Long-term follow-up of intrastromal corneal ring segments in keratoconus," J. Cataract Refract. Surg., vol. 35, no. 10, pp. 1768–1773, 2009, doi.org/10.1016/j.jcrs.2009.05.036.
[16] C. J. Roberts and W. J. Dupps Jr, "Biomechanics of corneal ectasia and biomechanical treatments," J. Cataract Refract. Surg., vol. 40, no. 6, pp. 991–998, 2014, doi.org/10.1016/j.jcrs.2014.04.013.
[17] M. A. Lago et al., "A new methodology for the in vivo estimation of the elastic constants that characterize the patient-specific biomechanical behavior of the human cornea," J. Biomech., vol. 48, no. 1, pp. 38–43, 2015, doi.org/10.1016/j.jbiomech.2014.11.009.
[18] R. Asher, A. Gefen, E. Moisseiev, and D. Varssano, "An Analytical Approach to Corneal Mechanics for Determining Practical, Clinically-Meaningful Patient-Specific Tissue Mechanical Properties in the Rehabilitation of Vision," Ann. Biomed. Eng., vol. 43, no. 2, pp. 274–286, 2015, doi: 10.1007/s10439-014-1147-9.
[19] M. A. Lago et al., "Patient-specific simulation of the intrastromal ring segment implantation in corneas with keratoconus," J. Mech. Behav. Biomed. Mater., vol. 51, pp. 260–268, 2015, doi.org/10.1016/j.jmbbm.2015.07.023.